Supporting information:

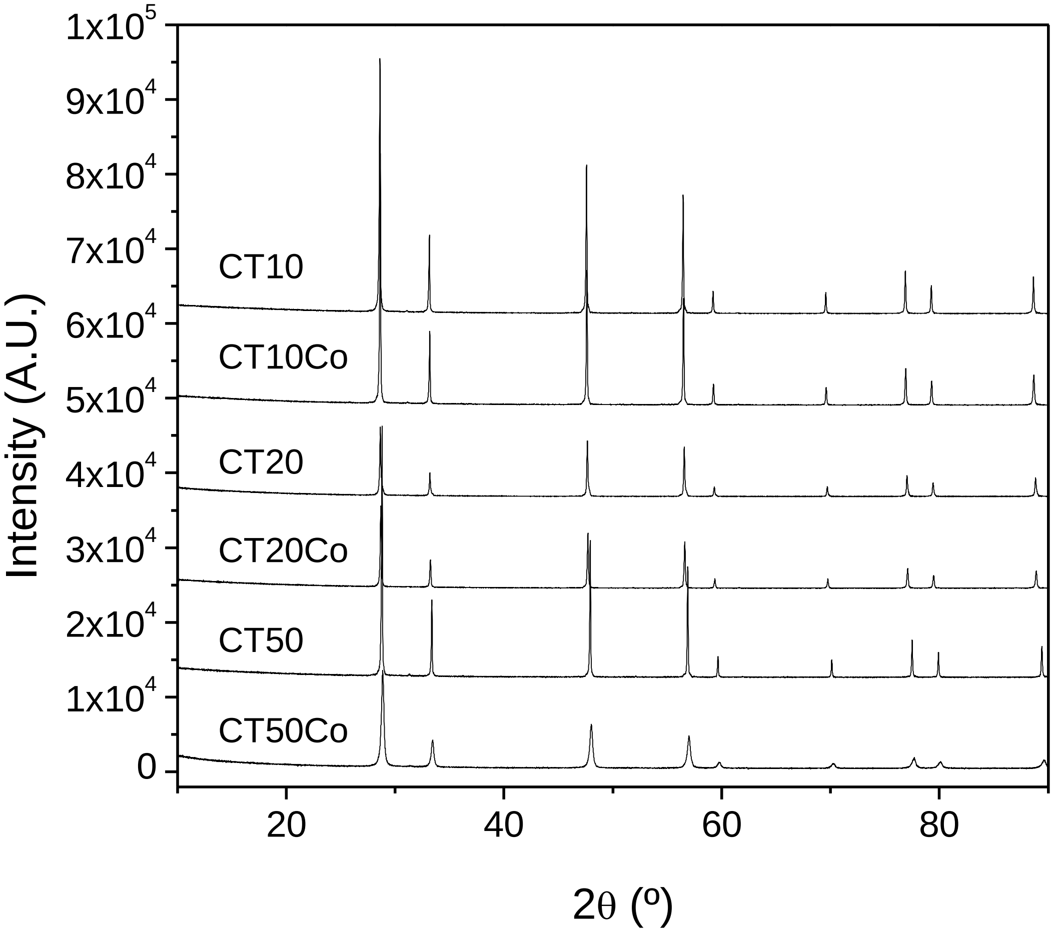

Figure S1. XRD patterns of the materials sintered at 1723 K. No impurity or secondary phases were observed up to the limit of the apparatus**.**

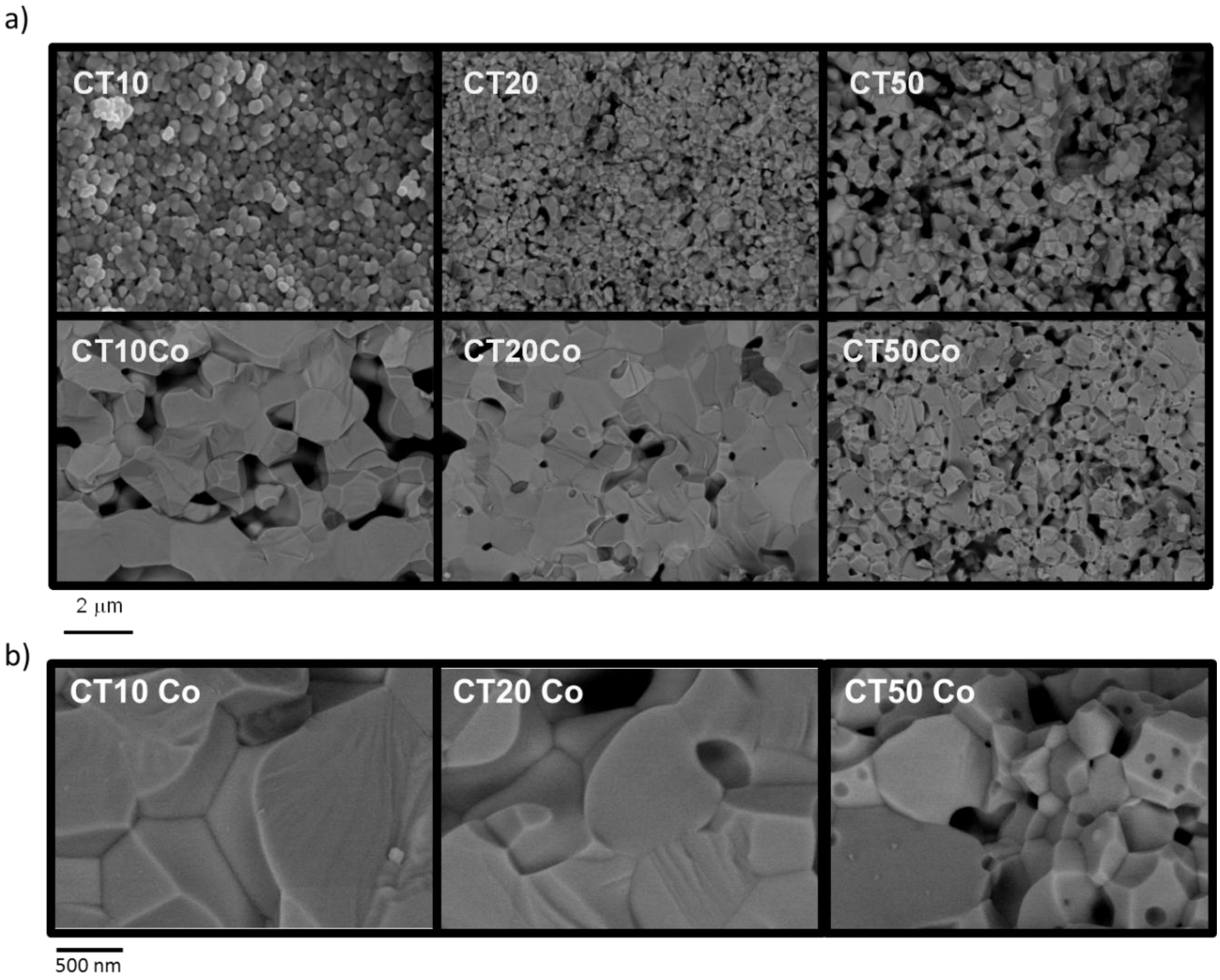

Figure S 2. a) Scanning microscope images of CTx and CTCox taken by backscatter electron detector, and b) grain boundary detail of the CTxCo samples.

Cobalt is a sintering aid that enables lowering the densification temperature. SEM pictures of CTx and CTxCo membranes showed in S1 show the grain size growth difference induced by the addition of cobalt. Dark CoO_x aggregates are observed, similarly to those observed for Pr-doped ceria and other reported doped cerias, as Gd-doped.

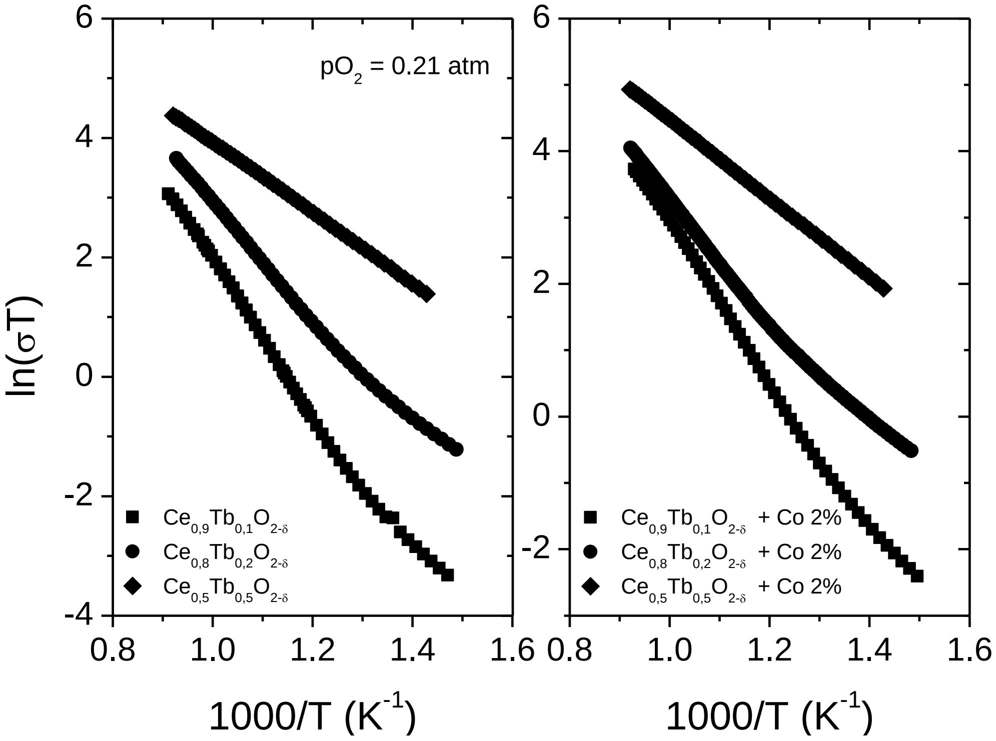

Figure S 3 . Arrhenius plot of the total conductivity in air for the Tb doped series.

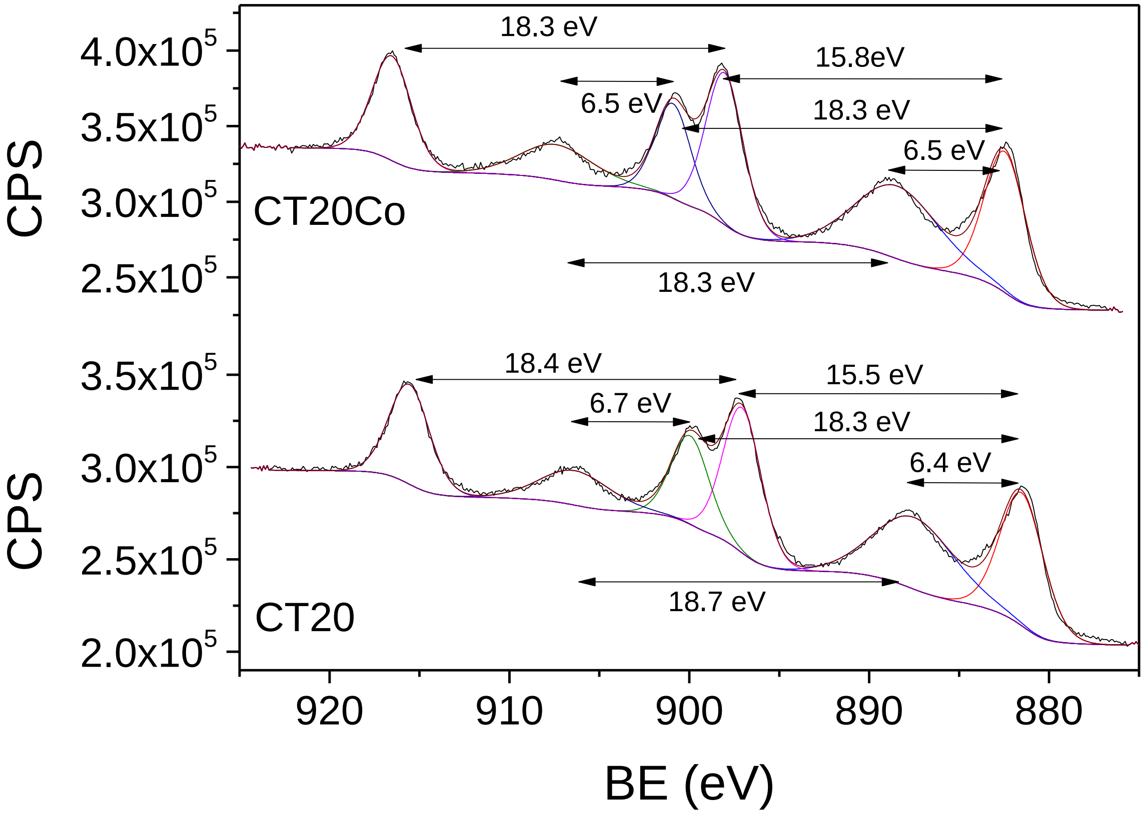

Figure S 4. Ce3d XPS spectra of CT20 and CT20Co. All the fitted peaks correspond to the Ce^{4+} oxidation state.

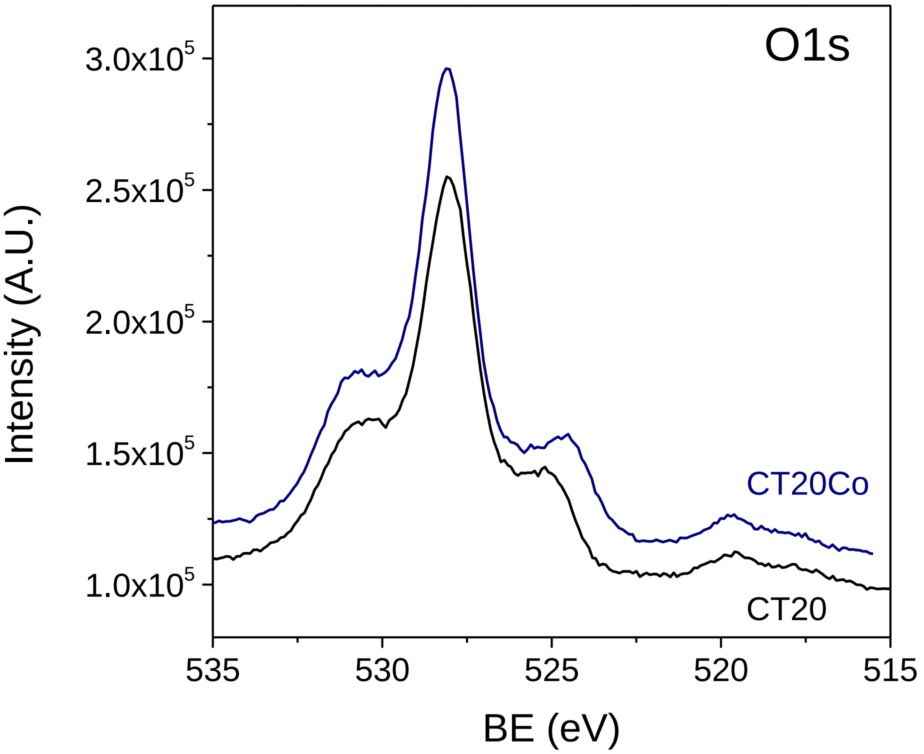

Figure S 5. O1s XPS spectra of CT20, CT20Co

Figure S4 depicts the O1s XPS spectra of CT20, CT20Co. They are principally composed of two components. The low energy peak observed at 528 eV is due to lattice oxygen and represents the existence of O^{2-}. The peak at higher binding energy 532 eV 530 eV is due to surface hydroxils (OH^-) and/or O^-, and carbonate groups. The hydroxyl groups are associated with Ce^{+3} ions located on the surface, therefore, the more intense peak at this region, the more number of Ce^{+3} ions [1]. The oxygen state at 525-524 eV does not change for the different samples since it arises from the sample holder and the oxygen from the chamber.

---

[1] Reddy B.M.;Katta L.; Thrimurthulu G. *Catalysis Today*, 2003, 83, 289.

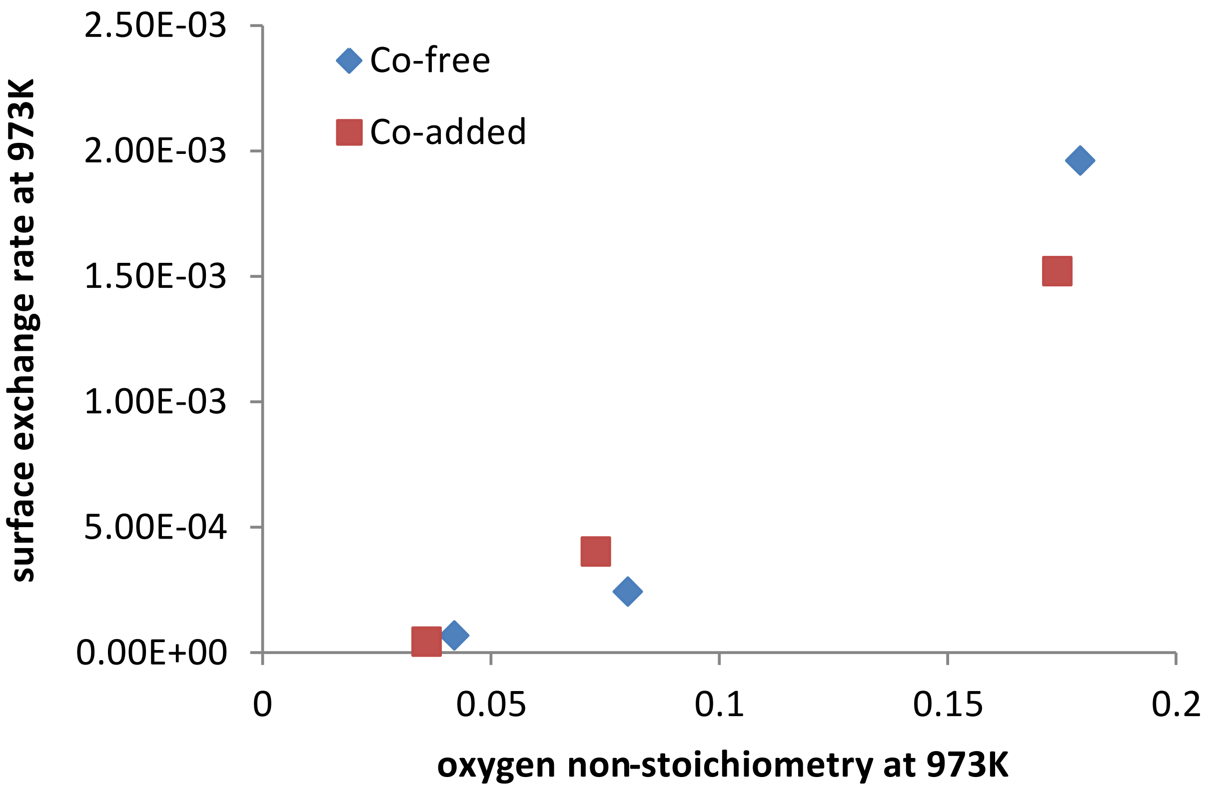

Figure S6. Surface exchange rate as a function of the oxygen non-stoichiometry at 973K

Co addition in 10 mol % Tb-doped ceria does not improve significantly $\Re_0$ with respect to the analogous sample without Co. However, the surface exchange rate exceeds that of the CT10 at temperatures above 750 ˚C. Above this temperature, the $[V_O^{\cdot\cdot}]$ reaches a maximum, i.e. Tb^{+3} is the prevailing Tb cation, as inferred from DC conductivity and TG experiments (Figure 3). Below 973 K surface exchange appears to be limited by the $[V_O^{\cdot\cdot}]$, partly due to the annihilation of oxygen vacancy associated with the partial oxidation of Tb from 3+ to 4+. However, when the Tb^{+4} starts to reduce at higher temperatures, $\Re_0$ is improved through Co addition, which slightly boost p-type conductivity.

Co addition to 20% mol doped ceria improves the surface exchange of oxygen with respect to the Co-free counterpart at any tested temperature. This behavior suggests that, for 20 mol% Tb doping, $[V_O^{\cdot\cdot}]$ was enough to ensure the reaction and the rate limiting step is the electronic contribution in this case. As a consequence, the increase in *p*-type conductivity by Co-addition alleviates the electronic limitation and raises the overall surface exchange rate. Table 1 shows the apparent $\Re_0$ activation energy obtained for all six compounds. The E_a observed for CT20Co decreases with respect to CT20, suggesting a possible change in the rate limiting step, presumably from limitation by insufficient electronic supply (CT20, 118 kJ/mol) to limitation by deficient $[V_O^{\cdot\cdot}]$

(CT20Co, 101 kJ/mol). Indeed, the E_a seemingly ascribed to $[V_O^{\cdot\cdot}]$ limitation coincides with the E_a observed for CT10 and CT10Co.

The surface exchange improvement through Co addition for CT20Co is not observed for the case of CT50Co. Indeed, E_a is not altered, which may indicate that there is no change in the rate limiting step when cobalt is added. Both CT50 and CT50Co showed high *p*-type electronic conductivity (Figure 3). Additionally, the E_a is similar to that observed for the samples limited by a process related to oxygen vacancies. Therefore, 50%-doped samples seem not to be limited by electronic supply but by a process in which oxygen vacancies play an important role. Accordingly, slightly higher exchange rates are observed for CT50, which can be explained by the fact that the non-stoichiometry of CT50 is a little higher than that for CT50Co (Figure S5).

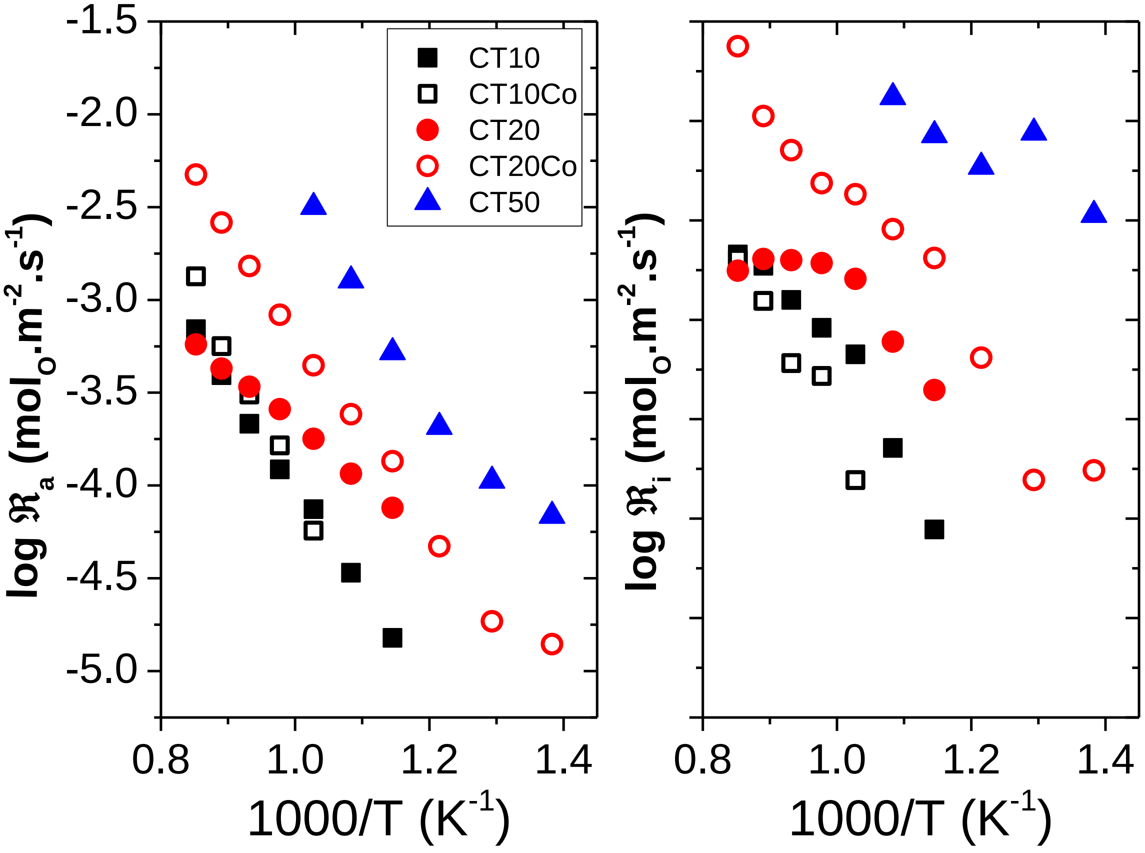

Figure S 7. Inverse temperature dependence of the rates of dissociative adsorption (ℜa), oxygen incorporation (ℜi) of the terbium doped studied series.

PIE experiments also provide information about the surface exchange mechanism. The isotopic exchange reaction has been modeled as a sequence of two steps, i.e. dissociative adsorption rate, $\Re_a$, and the incorporation of the oxygen into the ceria lattice, afterwards, $\Re_i$. Thus, overall exchange rate is considered to occur as a series process[2]. Figure S6 plots the rates of dissociative adsorption, $\Re_a$, and oxygen incorporation, $\Re_i$, as a function of the inverse temperature. The surface exchange process is controlled by the dissociative adsorption for all six samples as inferred from the fact that the $\Re_a$ is around one to two orders of magnitude lower than $\Re_i$, depending on the temperature.

---

[2] $$\frac{1}{\Re_o} = \frac{1}{\Re_a} + \frac{1}{\Re_i}$$